Liposome doxorubicin attenuates cardiotoxicity by reducing ferritinophagy

Yating Yu
Tianjin Medical University General Hospital
Haiyue Niu
Tianjin Medical University General Hospital
Mengying Zhang
Tianjin Medical University General Hospital
Mengyuan Liu
Tianjin Medical University General Hospital
Yue Zhang
Tianjin Medical University General Hospital
Jinyue Yang
Tianjin Medical University General Hospital
Yumei Liu
Tianjin Medical University General Hospital
Limin Xing
Tianjin Medical University General Hospital
Zonghong Shao
Tianjin Medical University General Hospital
Rong Fu
Tianjin Medical University General Hospital
Huaquan Wang (wanghuaquan@tmu.edu.cn)
Tianjin Medical University General Hospital

Research Article

Keywords: Doxorubicin-induced cardiotoxicity, Autophagy, Ferroptosis, Ferritinophagy, NCOA4

Posted Date: April 7th, 2023

DOI: https://doi.org/10.21203/rs.3.rs-2771665/v1

Abstract

Background

Doxorubicin (DOX) is widely used in lymphoma, myeloma, breast cancer, and other malignant tumors, and it significantly improves the prognosis of these patients. However, its side effects, especially cardiotoxicity, must be taken seriously. Studies have shown that liposome doxorubicin (L-DOX), compared with DOX, has increased anti-tumor activity and decreased cardiac toxicity. Our aim is to investigate the mechanism of myocardial injury in mice caused by these two drugs, to identify potential mitigation strategies.

Methods

In this study, mice or HL-1 cells were treated with DOX or L-DOX, and the cardiac morphology, hemodynamic effect, laboratory examination, and expression of ferritinophagy-related proteins were compared with the control group.

Results

DOX significantly induced myocardial cell death, while L-DOX had little effect on myocardial injury. Additionally, DOX significantly increased the level of autophagy and ferroptosis in cardiac myocytes. Further analysis revealed that NCOA4-mediated ferritinophagy played a key role in the mechanism of doxorubicin-induced cardiotoxicity (DIC). Importantly, the addition of ferrostatin-1 (a ferroptosis inhibitor) was able to rescue DIC. In contrast, L-DOX reduced the damage to cardiac myocytes by reducing ferritinophagy.

Conclusion

We have found that a significant relationship between the mechanism of DIC and NCOA4-mediated ferritinophagy. L-DOX has been shown to reduce the damage to myocardial cells by reducing NCOA4-mediated ferritinophagy. Thus, NCOA4 has the potential to be a drug target for the cardiac protection of DIC. However, further research is need to investigate the specific role of NCOA4 in the pathogenesis of DIC.

Introduction

Doxorubicin (DOX) is one of the first-line chemotherapy drugs for some tumors (such as lymphoma, leukemia, sarcoma, and breast cancer). Compared with tumor cells, cardiac myocytes are more sensitive to doxorubicin-induced oxidative stress because they are highly dependent on oxidative metabolism. In addition, its pharmacokinetics are characterized by a very short half-life in the cycle, with wide and non-

selective distribution. The tumor doxorubicin level in the mouse model is difficult to reach at the peak level of 2% of the tumor injection dose per gram (% ID/g) [1]. Therefore, like many other anticancer drugs, effective treatment with doxorubicin usually requires high doses, which may further aggravate the adverse toxic side effects due to the lack of selectivity of the drug.

Doxorubicin-induced cardiotoxicity (DIC) is always difficult to predict and it is the dose-limiting toxicity of doxorubicin. A study showed that the overall incidence of DIC was 9%, with cardiotoxicity occurring in 98% of cases within the first year. In addition, left ventricular ejection fraction (LVEF) and the cumulative dose of doxorubicin after chemotherapy are independent risk factors for cardiotoxicity [2]. Therefore, DIC will not only lead to a higher direct incidence rate and mortality, but also hinder the use of the most effective first-line cancer treatment. In current clinical practice, the conventional treatment for heart failure is as follows: β-receptor blockers and renin-angiotensin system inhibitors are effective, but they are unlikely to solve the specific molecular pathway leading to DIC.

DOX causes an increase in oxygen absorption and produces various types of reactive oxygen species (ROS), leading to oxidative stress [3]. The data showed that the generation of ROS induced by DOX could trigger the interruption of autophagy flux and mitochondrial oxidative damage, ultimately leading to lipid peroxide-dependent ferroptosis and many other types of regulatory cell death [5, 4]. In addition, some studies have shown that mitochondrial dependent ferroptosis plays a key role in the progression of DIC [6]. Therefore, autophagy and ferroptosis may be the important pathways leading to DIC. In recent years, there has been a lot of evidence that links between iron metabolism and autophagy. With the increase of intracellular autophagy levels, ferroptosis is also more likely to occur [7]. Nuclear acceptor activator 4 (NCOA4) is a selective cargo receptor that can regulate iron homeostasis by binding with ferritin and promoting its autophagy and degradation. This process is called “ferritinophagy” [8]. More and more studies suggest that NCOA4 can promote ferritinophagy by increasing intracellular free iron, glutathione production, and accumulation of ROS [9].

Compared with free (non-liposome) preparations, the liposome delivery system significantly improves the efficacy and safety of chemotherapy drugs. A liposome is a vesicle composed of a lipophilic bilayer and a hydrophilic core, which provides a perfect opportunity for it to be used as a carrier of various therapeutic and diagnostic agents. Polyethyleneglycolated (PEG) liposome doxorubicin is clinically approved, and Doxil® has proven the benefits of polyethylene glycol surface modification of liposomes [10]. The size of polyethylene glycol liposome doxorubicin is relatively small (80–90 nm), which can selectively pass through the endothelial cell window of tumor blood vessels and release doxorubicin at tumor sites, with the smallest release in plasma and healthy tissues. In addition, PEG coating provides a highly hydrophilic, protective, and flexible covering layer for liposomes, avoiding the detection of the mononuclear phagocyte system, thus prolonging the circulation time in the blood [11]. As shown in the clinical trial result, intravenous injection of polyethylene glycol liposome doxorubicin is an effective choice for the treatment of various malignant tumors, including metastatic breast cancer, ovarian cancer,

multiple myeloma, and AIDS-related Kaposi sarcoma. Compared with traditional doxorubicin and other available chemotherapy drugs, it has good safety [12].

Method

Animals

Male C57BL/6J mice were placed in a room with temperature and humidity control, fed a commercial diet, and provided with free access to water. The DIC model was pre-tested with reference to the previous report, and some modifications were made to the administration method. In brief, on the 1st and 8th day, DOX was administered to mice by intraperitoneal injection (12 mg/kg and 18 mg/kg, respectively). After inhaling an appropriate amount of isoflurane and being anesthetized, the mice underwent an ultrasonic examination. Following euthanasia using an excessive amount of pentobarbital, their hearts were removed and weighed. The mice were weighed before and after administration.

reagent

DOX was purchased from Topscience (China) and L-DOX was purchased from CSPC Pharmaceutical Group (China). Fer-1 was purchased from MedChemExpress (USA), and dimethyl sulfoxide (DMSO) was purchased from Sigma Chemical (USA). FeRhoNox-1 was purchased from GORYO Chemical (Japan); Fetal bovine serum (FBS) was purchased from Lonsera (Uruguay); The photosphatebuffered saline (PBS) solution was purchased from Beijing Solarbio Science & Technology Co.,Ltd(China).

Echocardiogram (ECG)

Echocardiographic data were obtained from two-dimensional target M-type images, which were acquired in a long-axis view at the papillary muscle level using the Vevo 2100 ultrasound system (Visual Sonics, Canada) under mild anesthesia (1–2% isoflurane).

Cell culture

HL-1 cells were cultured in DMEM supplemented with 10% fetal bovine serum (FBS), 100 μg/ml penicillin-streptomycin, and 2 mmol/L L-glutamine. To establish the DIC model, after the pre-experiment, the cells were cultured with a final concentration of 2 μmol/L of doxorubicin for 48 hours.

Cell viability analysis

Cell viability was determined by the CCK-8 assay (Yeasen Biotechnology, China). The cell suspension was inoculated in the 96-well plate and cultivated in a 37 °C, 5% CO_2 incubator for 24 hours. Then, the HL-1 cells were treated according to their assigned groups in a complete culture medium. Afterward, 10 μl CCK-8 reagent was added to each well and incubated for 4 hours. The absorbance at 450 nm was measured to calculate cell viability.

Western blot

We used GPX4 (Cell Signaling Technology, 52455), SLC7A11 (Cell Signaling Technology, 12691), LC3B (Cell Signaling Technology, 3868), NCOA4 (Abcam, ab86707), and β-actin (Bioss, bsm-33036M).

Real-time quantitative PCR (RT-PCR)

Total RNA was extracted using the Trizol method, and cDNA was synthesized through reverse transcription. After centrifuging the synthesized primer (Table 1), the corresponding volume of ddH_2O was added to dissolve it and dilute to a final concentration of 10 μmol/L. The samples were then stored in a refrigerator at -20 ℃. The 20μl PCR reaction system was prepared according to the instructions, and each sample was set with 3 compound wells before being placed into the PCR instrument for reaction.

Table 1
Primer sequence

gene	Forward	Reverse
BNP	CTGAAGGTGCTGTCCCAGATGATTC	GACTTCCCAGAGGATAGGAGTGACC
ANP	AAGAACCTGCTAGACCACCTGGAG	TGCTTCCTCAGTCTGCTCACTCAG
NCOA4	CTGTCTGATTGGTTGGTGACTCCTC	GGCTCTCTGAACACCTGGAACAAG
LC3B	CAAGCCTTCTTCCTCCTGGTGAATG	CCATTGCTGTCCCGAATGTCTCC
GPX4	TACGCTGAGTGTGGTTTGCG	CGCGGCGAACTCTTTGATCT
SLC7A11	ACGGTGGTGTGTTTGCTGTCTC	GCTGGTAGAGGAGTGTGCTTGC
ACSL4	GCTCTGTCACACACTTCGACTCAC	TTCCCTGGTCCCAAGGCTGTC
β-actin	GGCTGTATTCCCCTCCATCG	CCAGTTGGTAACAATGCCATGT

Histological analysis

For histological analysis, the apical myocardium was preserved in 4% paraformaldehyde for at least four days. It was then dehydrated, waxed, embedded, and stained with hematoxylin and eosin.

Determination of MDA by TBA method

The MDA concentration was determined using the TBA method as described in the MDA reagent kit instructions (Nanjing Jiancheng Bioengineering Institute, China). The reaction system was mixed thoroughly using a vortex mixer (Haimen Kylin-Bell Lab Instruments, China), and then cooled using running water after a water bath. Next, the mixture was centrifuged, and the supernatant was collected. The absorbance value of each hole was measured at 532 nm.

Determination of GSH by microplate method

GSH concentration was determined using the microplate method. After collection, the cells were washed with PBS and centrifuged at low speed of 1500 rpm for 5 minutes to obtain a cell pellet. The pellet was resuspended, and the resulting supernatant was used for the test. The reaction system was prepared

according to the instructions of the GSH reagent kit (Nanjing Jiancheng Bioengineering Institute, China). After mixing, the solution was allowed to stand for 5 minutes before measuring the absorbance value of each well at 405 nm.

Measurement of lipid peroxidation by C11-BODYPY 581/591

Lipid peroxidation was measured using C11-BODYPY 581/591 (Thermo Fisher Scientific). Briefly, HL-1 cells were incubated with C11-BODIPY581/591 at 37 ° C for 30 minutes following 48 hours of different interventions. After washing with PBS, fluorescence measurements were taken.

Flow cytometry analysis

The apoptosis of HL-1 cells was evaluated using the Annexin V-PI double staining method. Briefly, HL-1 cells were isolated and collected, and then stained with 5 μL FITC Annexin V and 5 μL PI (BD Pharmangen, USA). The cells were incubated in the dark at room temperature (25°C) for 15 minutes, and then resuspended within 1 hour for detection using flow cytometry (Beckman Company, USA).

Detection of Fe^{2+}

Intracellular Fe2 + was detected using FeRhoNox-1. HL-1 cells from different treatment groups were washed with HBSS and incubated with FeRhoNox-1 in HBSS (5 μmol/L) at room temperature in a humidified chamber for 60 minutes. After being washed three times with HBSS, the cells were observed using a fluorescence microscope (Leica, Germany).

Microarray datasets

In this study, the raw gene expression profiles GSE23598 and GSE59672 were downloaded from the GEO database (https://www.ncbi.nlm.nih.gov/geo/).The GSE23598 expression profile consists of two wild-type mice without DOX treatment and two wild-type mice with DOX treatment, which were detected using the Affymetrix Mouse Genome 430 2.0 Array. Similarly, the GSE59672 expression profile consists of three wild-type mice without DOX treatment and three wild-type mice with DOX treatment, detected using the same way.

Data processing

To extract key information from the two gene expression matrices, we used the AnoProbe package from R software (R-project. org) to process and group the data. The probe ID of each gene was converted into a gene symbol, and then the data was standardized using the limma package. Subsequently, we performed gene set enrich analysis (GSEA) on the data.

Statistics

Graphpad Prism 9.0 was used for statistical analysis and chart drawing. The data were presented as mean ± standard deviation (mean ± SD). For normally distributed data, we used the t-test (for two groups) or one-way analysis of variance (ANOVA) (for more than two groups). For non-normally distributed data,

we used nonparametric test. Pearson analysis was used for correlation analysis, and a *P*-value of < 0.05 was considered statistically significant.

Result

GSEA analysis showed that the autophagy pathway in DOX-treated mice was significantly up-regulated

To explore the possible mechanism and pathway of DIC in mice, two data sets (GSE5967 and GSE2359) were analyzed using GSEA. As expected, the results derived were highly correlated with autophagy. As an RNA-binding protein, the elevation of LC3B is related to autophagy activation[13]. Volcano map analysis of differential genes in the data set GSE5967 showed that LC3B gene was significantly up-regulated ($p < 0.01$) (Fig. 1C).

Construction of DIC model

In order to describe the characteristics of mouse DIC, we induced DIC in mice. The following pre-experiments were carried out in advance to determine the appropriate dosage: (1) NC group: each mouse was intraperitoneally injected with the same volume of normal saline on the 1st and 8th days. (2) Cumulative dose of 25mg/kg (25 PDOX): each mouse was injected intraperitoneally with 10 mg/kg and 15 mg/kg DOX, respectively, on the 1st and 8th day. (3) Cumulative dose of 30mg/kg (30 PDOX): each mouse was injected with 12 mg/kg and 18 mg/kg DOX, respectively, by intraperitoneal injection on the 1st and 8th day. (4) Cumulative dose of 35mg/kg (35 PDOX): each mouse was injected intraperitoneally with 15 mg/kg and 20 mg/kg DOX, respectively, on the 1st and 8th day. (5) Cumulative dose of 40 mg/kg (40 PDOX): each mouse was injected with 17 mg/kg and 23 mg/kg DOX respectively by intraperitoneal injection on the 1st and 8th day. Before the end of administration, the mortality of mice in the 35mg/kg group reached 50%, and the mortality of mice in the 40mg/kg group reached 100%. We observed weight loss of mice and the relative increase of cardiac mass, especially the relative increase in left ventricular mass (heart mass/weight, left ventricular mass/heart mass) (Fig. 2D E F G H). This indicates that DOX can cause wasting and myocardial atrophy in mice. However, compared to the degree of weight loss, the degree of cardiac mass loss is small, and the left ventricular hypertrophy is relatively thick, indicating that its cardiac insufficiency is caused by insufficient myocardial compensation. Since the left ventricular ejection fraction (LVEF) of the group with a cumulative dose of 30mg/kg decreased the most in echocardiography and all the mice survived, we chose this method of administration in the formal experiment (Fig. 2A B C). Moreover, we found that with the increase of the dose of doxorubicin, the GSH level of mouse cardiomyocytes decreased significantly (Fig. 2I).

Liposome doxorubicin-induced cardiac toxicity in vivo is lower than doxorubicin

We observed that the left ventricular ejection fraction (LVEF) and fractional shortening (FS) of the DIC model mice (P-DOX group) decreased, but there was no significant difference due to the small number of samples. However, the cardiac output (CO) of the DIC model mice decreased significantly ($p < 0.05$) (Fig. 2J KLM). The LVEF and FS of mice treated with the same dose of liposome doxorubicin also

showed a downward trend, but compared with DIC mice, the decline was smaller. In addition, histological analysis showed that the myocardial cells of DIC mice were atrophic, and the connections between myocardial cells were sparser (Fig. 3A). The levels of ANP and BNP, markers of myocardial injury, were significantly increased in the DOX group (Fig. 3D E).

DOX may induce autophagy of mouse cardiomyocytes

We evaluated whether autophagy and ferroptosis were involved in the process of DIC. As shown in the figure, the level of LC3B was significantly increased in mouse cardiomyocytes treated with DOX, both at the transcriptional level and the translational level, while the difference between L-DOX group and the control group was not significant (Fig. 3F K). All the above results showed that DOX significantly increased the level of LC3B, indicating that autophagy occurred, while L-DOX had a weak ability to induce autophagy in vivo.

DOX may induce ferritinophagy in mouse cardiomyocytes

Malondialdehyde (MDA) is one of the most commonly used biomarkers of oxidative stress [14]. The results showed that MDA increased in the myocardium of P-DOX mice. Glutathione (GSH) is an important member of the cellular antioxidant system. High levels of GSH can eliminate excessive ROS, while GSH depletion will lead to increased ROS and ferroptosis[15]. Our results showed that GSH was significantly depleted in the DOX treatment group, while no difference was observed in the L-DOX group (Fig. 3B C). The indicators SLC7A11 and GPX4, related to ferroptosis, were also significantly depleted in the DIC model, suggesting that ferroptosis may have occurred at the same time (Fig. 3I J). We also detected NCOA4, the key protein of ferritinophagy, whose expression was significantly increased in P-DOX group, indicating that ferritinophagy may have occurred (Fig. 3G L).

Myocardial death was related to lipid peroxidation in vitro

We used HL-1 cell to verify the mechanism of DIC in vitro. Firstly, we constructed a DIC model based on HL-1 cells. In order to simulate the cardiotoxicity of DIC in vivo, we treated them with a concentration of 2 μmol/L for 48 hours to construct a cell model of DIC (Fig. 4A B). Ferrostatin-1 (Fer-1) inhibits ferroptosis by reducing the level of mitochondrial ROS [16]. Pre-experiment indicated that at a concentration of 10 μmol/L, it had the best effect on improving cell activity (Fig. 4C). Under the light microscope, it was observed that the number of HL-1 cells treated with DOX decreased significantly, and they lost their original normal shape, becoming spherical or beaded, with a significant decrease in the number of adherent cells. After adding Fer-1, the number of cells increased, and beaded cells decreased. Compared with the control group, the number of cells treated with L-DOX also decreased, and individual cells turned into spherical suspension cells, but significantly improved compared to the DOX group (Fig. 4D). CCK-8 detection showed that the activity of cardiomyocytes after DOX treatment decreased significantly, while Fer-1 could reduce myocardial death. The activity of cardiomyocytes after L-DOX was significantly better than that of P-DOX group, which showed that when the same drug concentration was applied to cardiomyocytes, both of them had damage to cardiomyocytes, but L-DOX had less impact on them

(Fig. 4E). Annexin V-PI apoptosis analysis showed that apoptosis was not related to DIC (Fig. 4F G). Next, we used C11BODIPY to detect the level of lipid peroxidation in cardiac myocytes. The results showed that the level of lipid peroxidation in P-DOX group was significantly increased. Fer-1 could significantly reduce the level of lipid peroxidation in DOX, and the level of lipid peroxidation in DOX was also significantly higher than that in L-DOX (Fig. 4H I).

NCOA4-mediated ferritinophagy was up-regulated in HL-1 cells

We used a Fe^{2+} probe to detect the concentration of Fe^{2+} in the cytoplasm in vitro. We observed a significant increase in the concentration of Fe^{2+} in the cardiac cytoplasm after DOX treatment, which could be decreased by Fer-1. Moreover, we found that the concentration of Fe^{2+} in the cardiac cytoplasm after L-DOX treatment increased compared to the NC group, but decreased compared to the P-DOX group, with a statistical difference (Fig. 5A B). We also detected the levels of MDA and GSH in the HL-1 cells, which were similar to those in the in vivo experiments, indicating an increase in the level of ferroptosis in the HL-1 cell after DOX treatment. Fer-1 was found to reduce ferroptosis of myocardial cells (Fig. 5C D). Consistent with this, the mRNA levels of SLC7A11 and GPX4, which are related to ferroptosis, were significantly reduced in the DIC model (Fig. 5G H). Acyl-CoA synthetase long-chain family member 4 (ACSL4), a known ferroptosis promoter, also showed a significantly increased in transcription in DIC cell model (Fig. 5I) [17]. All the above results suggest a significant increase in the degree of ferroptosis in HL-1 cells after DOX treatment. The expression of LC3B, which represents the autophagy level, was significantly increased in the DIC cell model but not in the L-DOX group (Fig. 6E). In HL-1 cells, the expression of NCOA4 was significantly increased in P-DOX group and L-DOX group, with the expression level of P-DOX group being significantly higher than that of L-DOX group (Fig. 6D). These findings suggest that the mechanism of DIC and the mechanism of L-DOX causing less myocardial damage were closely related to ferritinophagy.

Discussion

Doxorubicin is currently used in various chemotherapy programs, but its excellent therapeutic effect is accompanied by cardiotoxicity [18]. DIC is difficult to predict and is the most common side effect that threatens the survival of patients. In the current research, the pathogenesis of DIC is different and includes autophagy, ferroptosis, and apoptosis[20, 19]. Currently, the cardiotoxicity induced by DOX can only be treated symptomatically [21].

Polyethylene glycol liposome doxorubicin is a type of doxorubicin that is wrapped by polyethylene glycol liposome. It prolongs drug's circulation time, enhances its accumulation in tumor tissue through passive targeting (enhancing permeability and retention effect), and reduces its cardiotoxicity while improving pharmacokinetic characteristics [10]. However, the specific pathway by which liposomal doxorubicin affects myocardial cells has not been reported compared to regular doxorubicin.

In this study, we investigated the effects of liposome doxorubicin(L-DOX) and regular doxorubicin (DOX) on myocardial cells in vitro and in vivo. After administering the same dose of drugs to mice, we found that L-DOX's toxicity on myocardial cells was significantly lower than DOX's, mainly observed through echocardiography and H&E staining. Furthermore, the transcription levels of ANP and BNP increased in the P-DOX group. Based on our analysis of the GEO database's results, we found that the autophagy pathway was significantly upregulated in cardiac myocytes after DOX administration. We measured autophagy-related indicators and found that the LC3B levels increased in mouse cardiomyocytes treated with DOX, but the difference between L-DOX group and control group was not significant. Our results suggest that DOX-induced myocardial death may be related to autophagy, while L-DOX-induced autophagy is weak.

Next, we found that MDA, which represents lipid peroxidation, increased in the DIC mice, while GSH was depleted in the DOX treatment group, but no difference was observed in the L-DOX group. Previous studies have shown that patients with DIC have a significantly higher cardiac mitochondrial iron level than those with other types of cardiomyopathy or normal cardiac function. Therefore, DIC's mechanism is caused by the accumulation of mitochondrial iron. Reducing the mitochondrial iron level can prevent DIC [22]. Ferroptosis is a newly discovered regulatory cell death characterized by the production of reactive oxygen species from accumulated iron and lipid peroxidation. Therefore, we suspect that DIC's mechanism is not only related to autophagy, but also closely related to ferroptosis. We measured ferroptosis-related indicators such as SLC7A11 and GPX4, and found that they were also significantly depleted in the DIC model, suggesting that ferroptosis might occur simultaneously.

Recent studies have shown that increased autophagy can degrade ferritin, increase iron level, and trigger oxidative damage caused by Fenton reaction [23]. NCOA4 is a cargo receptor for ferritin selective autophagic conversion (i.e. ferritinophagy), which has been proved to mediate the autophagic degradation of ferritin. Overexpression of NCOA4 will increase the degradation of ferritin, thus promoting ferroptosis. The level of $Fe^{2+}$and MDA in NCOA4 knockout cells decreased, while the content of $Fe^{2+}$and MDA in NCOA4 overexpression cells increased. In addition, the level of glutathione (GSH) in NCOA4 knockout cells increased, while the level of GSH in NCOA4 overexpression cells decreased [7]. These findings provide new insights into the interaction between autophagy and ferroptosis. Our results are also in line with these expectations. The expression of NCOA4 in mouse cardiomyocytes after DOX treatment was significantly increased, while the change in L-DOX group was not significant. Based on the results of in vivo experiments, we hypothesized that doxorubicin-induced cardiac death triggered autophagic ferroptosis.

Subsequently, we constructed an in vitro model of DIC using HL-1 cell, and used an appropriate concentration of Fer-1 to rescue DOX-induced myocardial injury. Under the light microscope, it was observed that the number of HL-1 cells decreased after incubation with DOX, and the long fusiform adherent cells changed into round non-adherent cells. Fer-1 was able to rescue the myocardial toxicity caused by DOX. In contrast, the number and morphology of cells in the L-DOX group also changed, but both changes were not significant. Apoptosis analysis showed that at the IC50 concentration, apoptosis

was not the main mechanism leading to HL-1 cells death. Next, we measured the level of lipid peroxidation in myocardial cells. The results showed that the level of lipid peroxidation in HL-1 cells was significantly increased after DOX treatment. Fer-1 could significantly reduce the level of lipid peroxidation induced by DOX, and the level of lipid peroxidation was significantly higher in the DOX group than that in the L-DOX group. We used a Fe^{2+} probe to detect the concentration of Fe^{2+} in the cytoplasm of HL-1 cells in vitro. It was observed that the concentration of Fe^{2+} in the cytoplasm of HL-1 cells treated with DOX increased significantly, and the concentration of Fe^{2+} in the cytoplasm of the cells treated with Fer-1 decreased. At the same time, it was also found that the concentration of Fe^{2+} in the cytoplasm of myocardial cells treated with L-DOX increased compared to the control group, but decreased compared to the DOX group, and there was a statistical difference. We also detected the level of MDA, GSH and the transcription of SLC7A11, GPX4 and ACSL4 in the HL-1 cells, indicating that the level of ferroptosis increased after DOX treatment. At the same time, the expression of LC3B, which represents autophagy level, was significantly increased in the DIC cell model, but not in L-DOX group. Next, we measured NCOA4 and found that its level increased in both DOX and L-DOX group. Based on the above results, ferritinophagy may have occurred.

In this study, we have confirmed that the mechanism of DIC is related to the ferritinophagy induced by NCOA4, and the mechanism of L-DOX causing less myocardial damage is also related to this pathway. By comparing in vivo and in vitro experiments, we have discovered an intriguing phenomenon. Specifically, in vivo experiments, the level of most indicators in the L-DOX group was similar to that in the control group. In vitro experiments, however, we observed significant differences between the L-DOX group and the P-DOX group, as well as between the L-DOX group and the control group.

Previous research has indicated that compared with DOX, L-DOX was larger in volume and cannot penetrate the tightly continuous capillary lining of myocardial microvessels, thus preventing the arrival of L-DOX and reducing damage to myocardial cells [11]. Additionally, liposome drug carriers can control and slow down the drug release in blood and tissues, thereby reducing the level of free drugs in plasma. Consequently, at the same dose, the amount of L-DOX enters the hearts of mice through the circulatory system is smaller, resulting in lower cardiac toxicity. However, in vitro experiments did not have the same blocking effect on macromolecules by the vascular wall, and thus, both L-DOX and DOX were exposed to HL-1 cells at the same time, resulting in increased cytotoxicity.

Conclusions

In conclusion, the mechanism of DIC is closely related to NCOA4-mediated ferritinophagy. The reduced cardiotoxicity caused by L-DOX, in comparison to DOX, can be attributed to two main factors: the polyethylene glycol liposome coat and the reduction of ferritinophagy (Fig. 7). Although the up-regulation of L-DOX ferritinophagy-related genes is minimal, caution is still advised in their use. Hence, in terms of clinical application, it is recommended that all patients undergo primary prevention of cardiotoxicity and closely monitor cardiac function during anti-cancer treatment.

Abbreviations

DOX: Doxorubicin

L-DOX: liposome doxorubicin

DIC: doxorubicin-induced cardiotoxicity

Fer-1: ferrostatin-1

NCOA4: Nuclear acceptor activator 4

LVEF: left ventricular ejection fraction

ROS: reactive oxygen species

PEG: Polyethyleneglycolated

PBS: photosphatebuffered saline

FBS: fetal bovine serum

GSEA: gene set enrich analysis

FS: fractional shortening

MDA: Malondialdehyde

GSH: Glutathione

GPX4: glutathione peroxidase 4

ACSL4: Acyl-CoA synthetase long-chain family member 4

Declarations

Availability of data and materials

The datasets used and/or analyzed during the current study are available from the corresponding author on reasonable request.

Acknowledgement

Not applicable.

Funding

This work was supported in part by by The National Natural Science Foundation of China (No.82270139), Key Technology Research and Development Program of Tianjin China (18ZXDBSY00140), Scientific research project funded by Tianjin Association of Medical and Health (tjsyljkxh016), Tianjin Key Medical Discipline(Specialty) Construction Project, General project funded by Tianjin Municipal Education Commission(2022KJ235), Beijing Cancer Prevention &Treatment Society(IZXUEYANZI2021-1009).

Authorship

Contribution: Y.Y., H.N., and M.Z. performed research and analyzed the data; H.W. designed studies, ensure the correct analysis of the data and drafted the manuscript; M.L., Y.Z., J.Y., Y.L., L.X., Z.S. and R.F. assisted in design research, oversaw data collection, and contributed to the writing of the manuscript. All authors carefully revised the manuscript and finally approved the manuscript.

Ethical Approval

The animal experiment conduction in this study were approved by the Ethics Committee of Tianjin Medical University.

Conflict-of-interest disclosure

The authors declare no competing financial interests.

References

1. Gabizon A, Chemla M, Tzemach D, et al. Liposome longevity and stability in circulation: effects on the in vivo delivery to tumors and therapeutic efficacy of encapsulated anthracyclines[J]. Journal of Drug Targeting, 1996, 3(5): 391–398.
2. Cardinale D, Colombo A, Bacchiani G, et al. Early detection of anthracycline cardiotoxicity and improvement with heart failure therapy[J]. Circulation, 2015, 131(22): 1981–1988.
3. Kong C-Y, Guo Z, Song P, et al. Underlying the Mechanisms of Doxorubicin-Induced Acute Cardiotoxicity: Oxidative Stress and Cell Death[J]. International Journal of Biological Sciences, 2022, 18(2): 760–770.
4. Fang X, Wang H, Han D, et al. Ferroptosis as a target for protection against cardiomyopathy[J]. Proceedings of the National Academy of Sciences of the United States of America, 2019, 116(7): 2672–2680.
5. Li D L, Wang Z V, Ding G, et al. Doxorubicin Blocks Cardiomyocyte Autophagic Flux by Inhibiting Lysosome Acidification[J]. Circulation, 2016, 133(17): 1668–1687.
6. Tadokoro T, Ikeda M, Ide T, et al. Mitochondria-dependent ferroptosis plays a pivotal role in doxorubicin cardiotoxicity[J]. JCI insight, 2020, 5(9): e132747, 132747.
7. Hou W, Xie Y, Song X, et al. Autophagy promotes ferroptosis by degradation of ferritin[J]. Autophagy, 2016, 12(8): 1425–1428.

8. Santana-Codina N, Mancias J D. The Role of NCOA4-Mediated Ferritinophagy in Health and Disease[J]. Pharmaceuticals (Basel, Switzerland), 2018, 11(4): 114.
9. Bellelli R, Federico G, Matte' A, et al. NCOA4 Deficiency Impairs Systemic Iron Homeostasis[J]. Cell Reports, 2016, 14(3): 411–421.
10. Makwana V, Karanjia J, Haselhorst T, et al. Liposomal doxorubicin as targeted delivery platform: Current trends in surface functionalization[J]. International Journal of Pharmaceutics, 2021, 593: 120117.
11. Gabizon A A, Patil Y, La-Beck N M. New insights and evolving role of pegylated liposomal doxorubicin in cancer therapy[J]. Drug Resistance Updates: Reviews and Commentaries in Antimicrobial and Anticancer Chemotherapy, 2016, 29: 90–106.
12. Ka L-W, St D, Gm K. Pegylated liposomal doxorubicin: a guide to its use in various malignancies[J]. BioDrugs : clinical immunotherapeutics, biopharmaceuticals and gene therapy, BioDrugs, 2013, 27(5).
13. Hwang H J, Ha H, Lee B S, et al. LC3B is an RNA-binding protein to trigger rapid mRNA degradation during autophagy[J]. Nature Communications, 2022, 13(1): 1436.
14. Tsikas D. Assessment of lipid peroxidation by measuring malondialdehyde (MDA) and relatives in biological samples: Analytical and biological challenges[J]. Analytical Biochemistry, 2017, 524: 13–30.
15. Niu B, Liao K, Zhou Y, et al. Application of glutathione depletion in cancer therapy: Enhanced ROS-based therapy, ferroptosis, and chemotherapy[J]. Biomaterials, 2021, 277: 121110.
16. L S, H W, S Y, et al. Herceptin induces ferroptosis and mitochondrial dysfunction in H9c2 cells[J]. International journal of molecular medicine, Int J Mol Med, 2022, 49(2).
17. Y W, M Z, R B, et al. ACSL4 deficiency confers protection against ferroptosis-mediated acute kidney injury[J]. Redox biology, Redox Biol, 2022, 51.
18. Rawat P S, Jaiswal A, Khurana A, et al. Doxorubicin-induced cardiotoxicity: An update on the molecular mechanism and novel therapeutic strategies for effective management[J]. Biomedicine & Pharmacotherapy = Biomedecine & Pharmacotherapie, 2021, 139: 111708.
19. Y W, X L, X W, et al. atg7-Based Autophagy Activation Reverses Doxorubicin-Induced Cardiotoxicity[J]. Circulation research, Circ Res, 2021, 129(8).
20. He H, Wang L, Qiao Y, et al. Epigallocatechin-3-gallate pretreatment alleviates doxorubicin-induced ferroptosis and cardiotoxicity by upregulating AMPKα2 and activating adaptive autophagy[J]. Redox Biology, 2021, 48: 102185.
21. Asnani A. Activating Autophagy to Prevent Doxorubicin Cardiomyopathy: The Timing Matters[J]. Circulation Research, 2021, 129(8): 801–803.
22. Ichikawa Y, Ghanefar M, Bayeva M, et al. Cardiotoxicity of doxorubicin is mediated through mitochondrial iron accumulation[J]. The Journal of Clinical Investigation, 2014, 124(2): 617–630.

23. Santana-Codina N, Del Rey M Q, Kapner K S, et al. NCOA4-Mediated Ferritinophagy Is a Pancreatic Cancer Dependency via Maintenance of Iron Bioavailability for Iron-Sulfur Cluster Proteins[J]. Cancer Discovery, 2022, 12(9): 2180–2197.

Figures

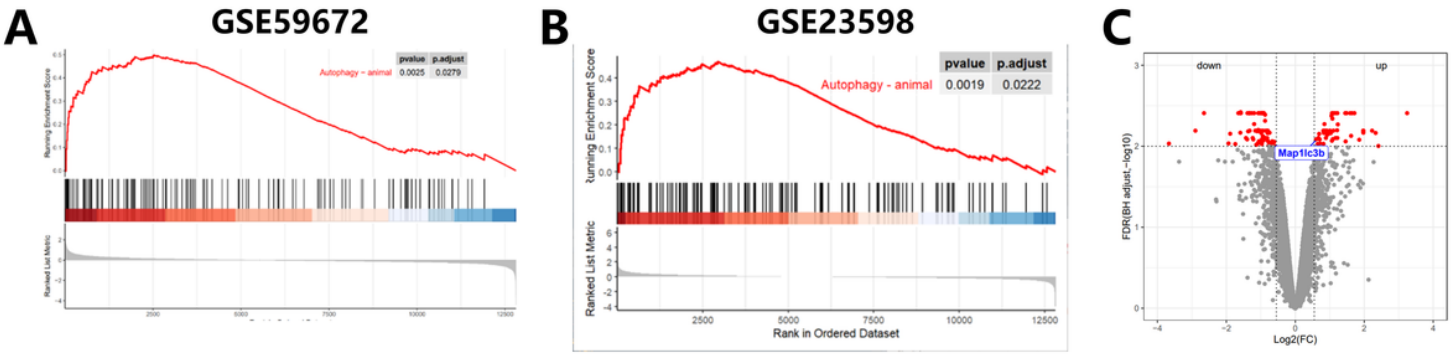

Figure 1

The analysis of two data sets in the GEO database. **(A)** GSEA analysis of data set GSE5967. **(B)** GSEA analysis of data set GSE5967. **(C)** Volcano map of differential genes in data set GSE5967.

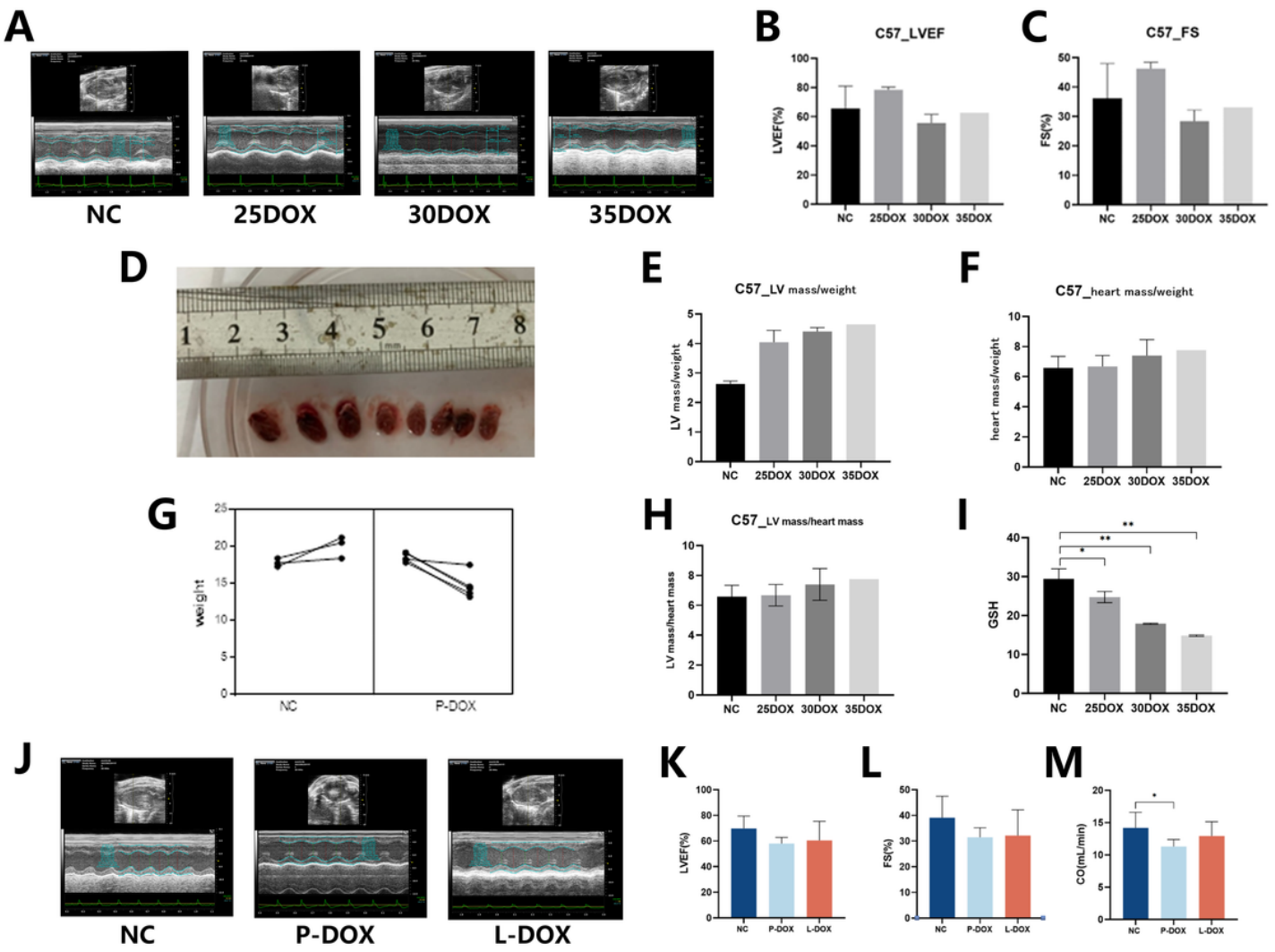

Figure 2

Results of pre-experiment. Grouping is carried out as described in "Construction of DIC model". **(A)**Transpapillary muscle section echocardiography(ECG) of mice in each group. **(B)** Ejection fraction and **(C)** fractional shortening according to the analysis of ECG. **(D)** Macroscopic view of mouse heart. **(E)** The ratio of left ventricular mass to weight of mice. **(F)** The ratio of heart mass to weight in mice. **(H)** The ratio of left ventricular mass to heart mass in mice. **(G)** Changes in body weight of mice before and after administration. **(I)** GSH level in myocardial cells. **(J)** ECG of mice in each group. Group: NC group: each mouse was intraperitoneally injected with the same volume of normal saline on the 1st and 8th day. P-DOX group: each mouse was intraperitoneally injected with 12 mg/kg and 18 mg/kg DOX respectively on the 1st and 8th day. L-DOX group: each mouse was injected intraperitoneally with 12 mg/kg and 18 mg/kg liposome doxorubicin(L-DOX) respectively on the 1st and 8th day. ECG parameters: **(K)** Left ventricular ejection fraction(LVEF). **(L)** Fractional shortening(FS). **(M)** Cardiac output(CO). The data are expressed as the mean ± SD of independent experiments. The differences were evaluated using one-way ANOVA. When $p<0.05$, the significance is verified (*).

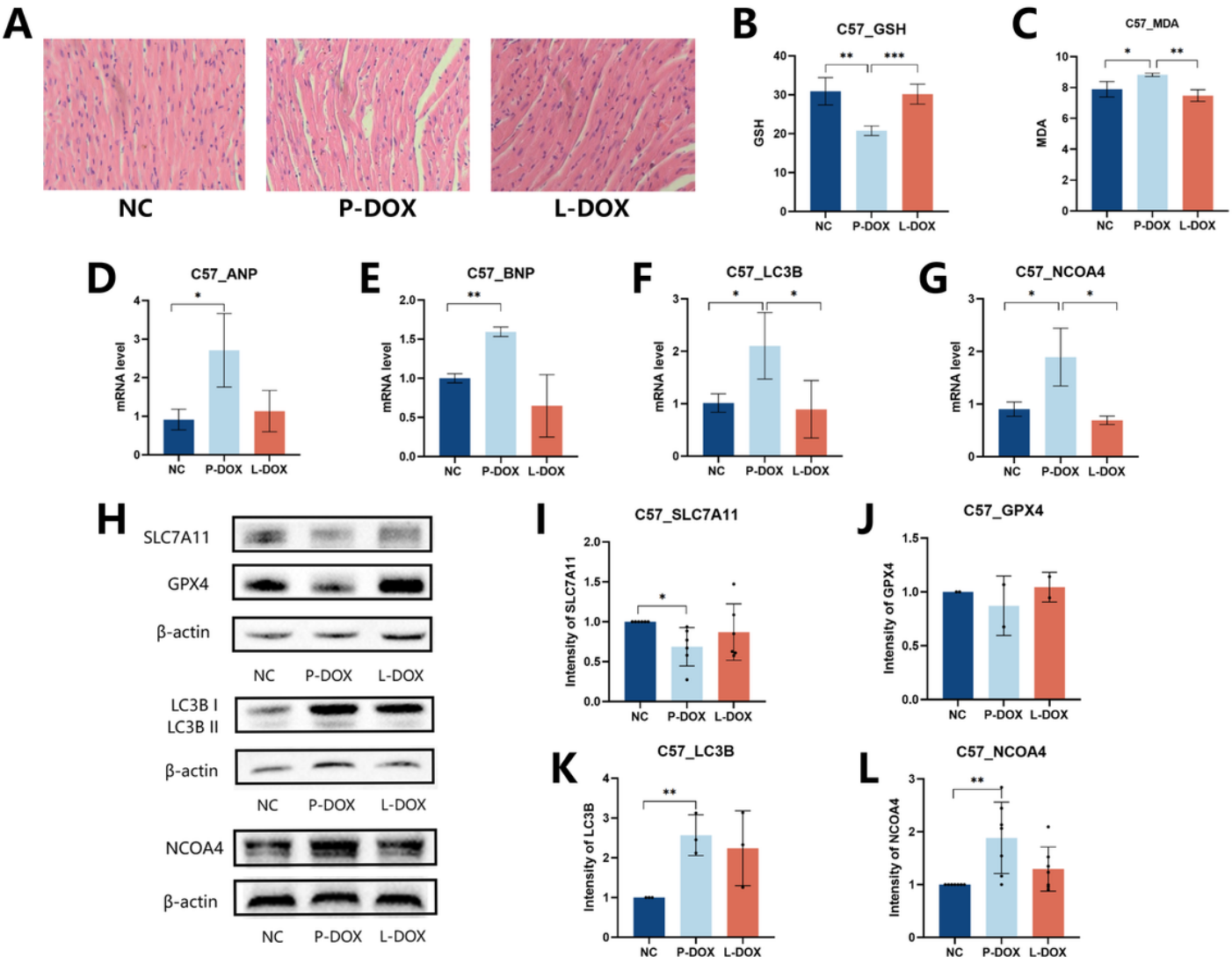

Figure 3

The results of DOX and L-DOX in vivo experiments show that DIC may be caused by ferritinophagy. (A) H&E staining of mouse heart tissue after DOX and L-DOX treatment. The levels of **(B)** GSH and **(C)** MDA in mouse cardiomyocytes after treatment with DOX and L-DOX. The mRNA levels of **(D)** ANP, **(E)**BNP, **(F)** LC3B, **(G)** NCOA4 in mouse cardiomyocytes after treatment with DOX and L-DOX. **(H)** Western blot assays was used to detect the expression of autophagy and ferritinophagy related proteins in cardiomyocytes treated with DOX and L-DOX. The relative intensity of SLC7A11 **(I)**, GPX4 **(J)**, LC3B **(K)**, NCOA4 **(L)** are shown in the histogram. The differences were evaluated using one-way ANOVA. When $p<0.05$, the significance is verified (*).

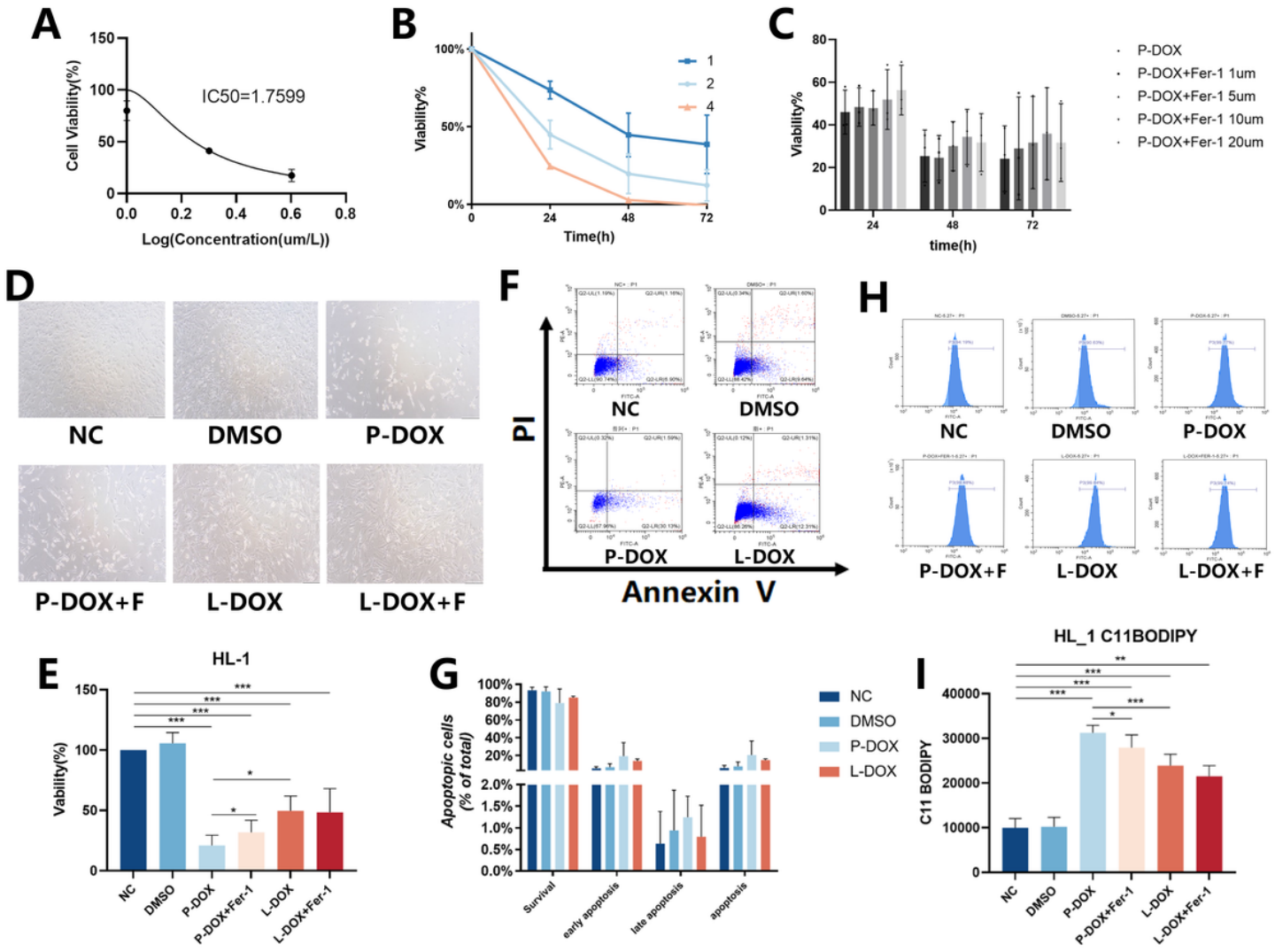

Figure 4

In vitro experiments showed that the mechanism of DIC was not related to apoptosis, but the level of lipid peroxidation was significantly increased. **(A)** The concentration-survival curve of DOX on HL-1 cell was determined by CCK-8 assay. The semi-inhibitory concentration (IC50) was 1.7599 μmol/L according to the curve. **(B)** CCK-8 assay was used to determine the survival curve of HL-1 cell when the concentration of DOX was 1μmol/L, 2μmol/L and 4μmol/L, respectively. **(C)** The cell viability of Fer-1 at different concentrations (1μmol/L,5μmol/L,10μmol/L,20μmol/L) was determined by CCK-8 assay. At Fer-1 concentration of 10μmol/L, the reversion of cell viability was the greatest. **(D)** The morphology of HL-1 cell was observed under light microscope. **(E)** CCK-8 assay was used to determine the cell viability of control group, DMSO group, P-DOX group, P-DOX+Fer-1 group, L-DOX group, L-DOX+Fer-1 group. **(F)**, **(G)** Apoptosis of HL-1 cells treated with DOX and L-DOX was measured by Annexin V/PI staining flow cytometry. **(H)**, **(I)** C11BODIPY to determine the level of lipid peroxidation between different groups. The differences were evaluated using one-way ANOVA. When $p<0.05$, the significance is verified (*).

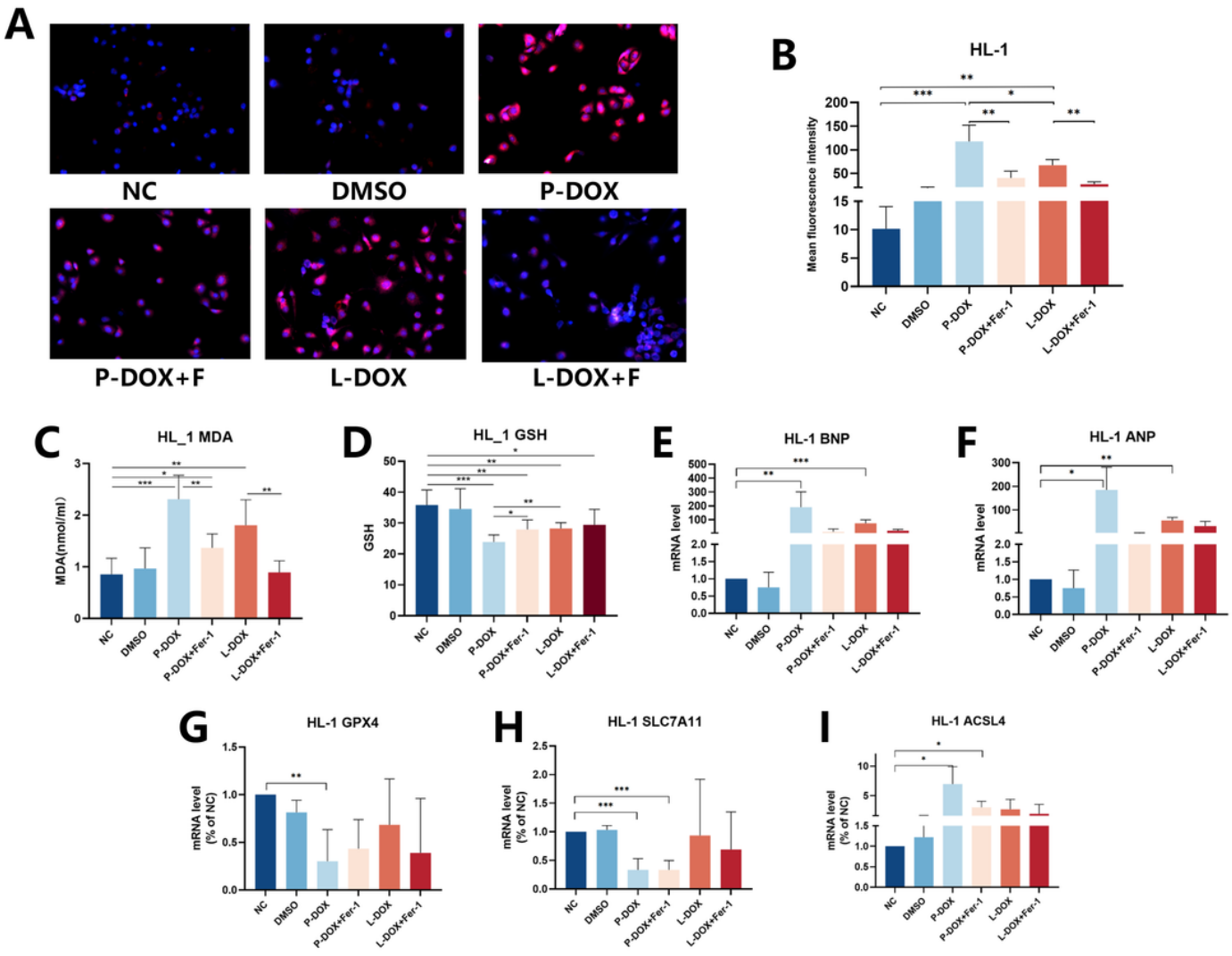

Figure 5

In vitro experiments showed that HL-1 cells were overloaded with iron and the level of ferroptosis increased after treatment with DOX, while the degree of iron overload caused by L-DOX was lower. **(A)** The intracellular Fe^{2+} in HL-1 cells were observed by fluorescence microscopy. FeRhoNox-1 is an activated fluorescent probe that can detect unstable Fe^{2+} through orange (red) fluorescence. DAPI, 4,6-diamino-2-phenylindole, a blue fluorescent nucleic acid stain, preferentially stains double-stranded DNA (dsDNA). **(B)** The orange fluorescence intensity was statistically analyzed. The levels of **(C)** GSH and **(D)** MDA in HL-1 cells after treatment with DOX and L-DOX with or without Fer-1. The mRNA levels of myocardial injury associated protein **(E)** ANP, **(F)** BNP, and ferroptosis associated protein **(G)** GPX4, **(H)** SLC7A11, **(I)** ACSL4 in HL-1 cells were detected by PCR. The differences were evaluated using one-way ANOVA. When $p<0.05$, the significance is verified (*).

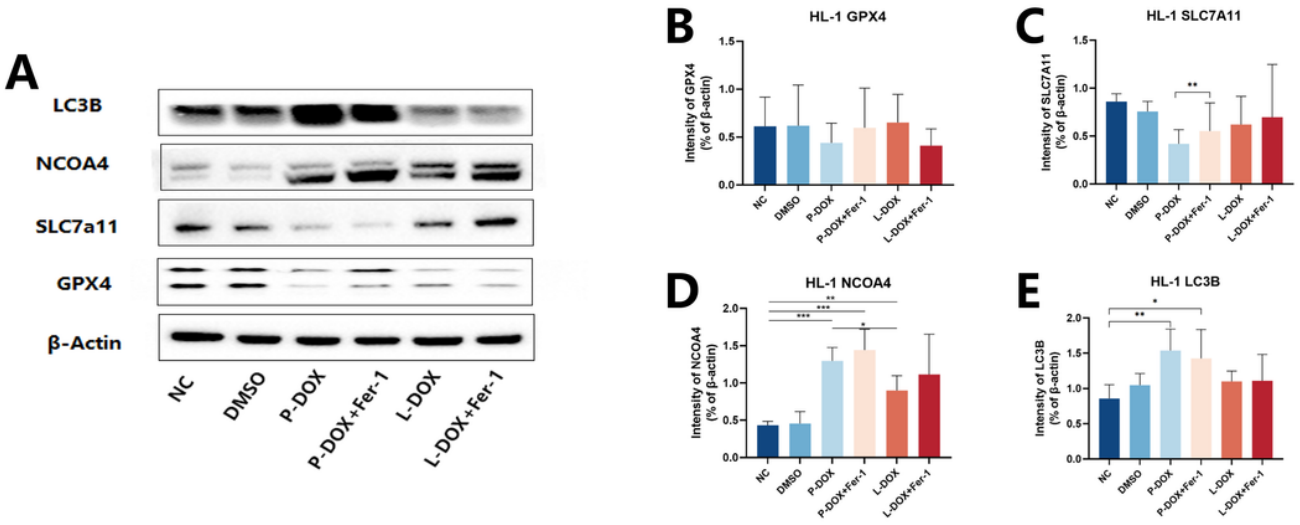

Figure 6

The level of NCOA4-mediated ferritinophagy in HL-1 cell was significantly increased after DOX treatment. Compared with DOX, the level of ferritinophagy in L-DOX treatment group was significantly decreased. **(A)** Western blot was used to detect the expression of ferroptosis, autophagy and ferritinophagy related proteins in HL-1 cells. The relative intensity of expression level of GPX4 **(B)**, SLC7A11 **(C)**, NCOA4 **(D)** and LC3B **(E)** are shown in the histogram. The differences were evaluated using one-way ANOVA. When $p<0.05$, the significance is verified (*).

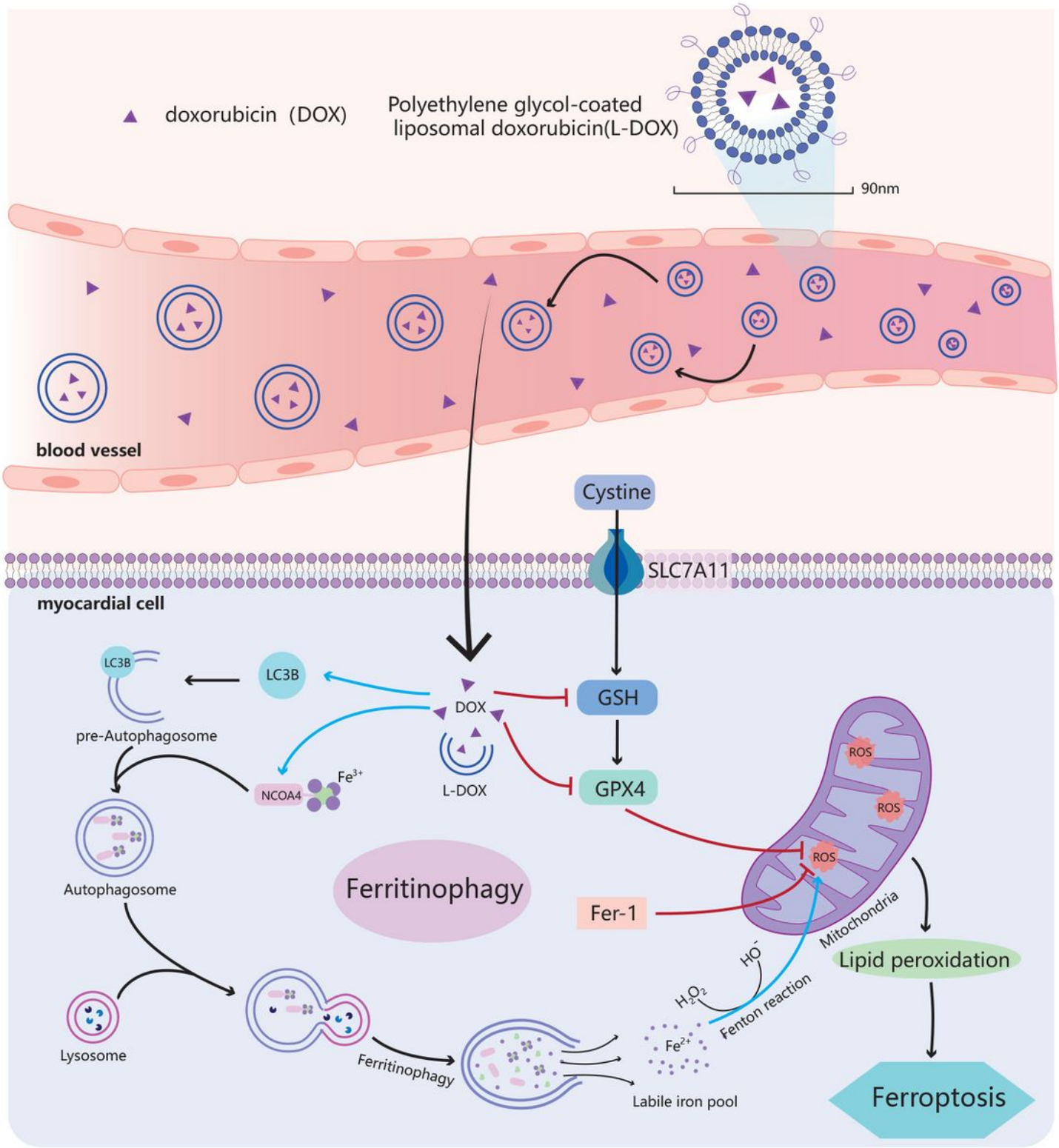

Figure 7

Role of DOX and L-DOX in ferritinophagy-related cardiomyocyte death. Both DOX and L-DOX reach the target organ through blood circulation. L-DOX is large in volume and cannot pass through the tightly continuous capillary lining of myocardial microvessels. L-DOX can maintain the complete structure in the plasma, so it has longer time in blood circulation and less damage to the tissue. In cardiomyocyte, DOX induces an increase in the expression of LC3B and forms a pre-autophage. NCOA4 releases free Fe^{2+}

through binding with ferritin and promoting its autophagic degradation. Fe^{2+} causes an increase in reactive oxygen species (ROS) through Fenton reaction. On the other hand, DOX can deplete GSH and GPX4 to increase ROS level. With the increase of ROS level, the level of lipid peroxidation will also increase, eventually leading to myocardial injury.